STRUCTURAL CONTROL AND HEALTH MONITORING
Struct. Control Health Monit. 2010; **17**:808–824
Published online 25 August 2010 in Wiley Online Library
(wileyonlinelibrary.com). DOI: 10.1002/stc.415

Market-based frequency domain decomposition for automated mode shape estimation in wireless sensor networks

Andrew T. Zimmerman and Jerome P. Lynch*,†

Department of Civil and Environmental Engineering, University of Michigan, 2350 Hayward St, 2380 G.G. Brown Building, Ann Arbor, MI, U.S.A.

SUMMARY

Wireless sensing technology has paved the way for the cost-effective deployment of dense networks of sensing transducers within large structural systems. By leveraging the embedded computing power residing within networks of wireless sensors, it has been shown that powerful data analyses can be performed autonomously and in-network, without the need for central data processing. In this study, the power and flexibility of agent-based data processing in the wireless structural monitoring environment is illuminated through the application of market-based techniques to in-network mode shape estimation. Specifically, by drawing on previous wireless sensor work in both decentralized frequency domain decomposition (FDD) and market-based resource allocation, an algorithm derived from free-market principles is developed through which an agent-based wireless sensor network can autonomously and optimally shift emphasis between improving the accuracy of its mode shape calculations and reducing its dependency on any of the traditional limitations of wireless sensor networks: processing time, storage capacity, and power consumption. The developed algorithm is validated by estimating mode shapes using a network of wireless sensors deployed on the mezzanine balcony of Hill Auditorium located at the University of Michigan.

KEY WORDS: structural health monitoring; wireless sensor networks; distributed data processing; agent-based systems; frequency domain decomposition; modal identification

1. INTRODUCTION

The introduction of wireless communications in the structural monitoring setting has made structural monitoring systems more pervasive, reliable, and affordable. Specifically, wireless telemetry allows traditionally long and expensive runs of coaxial cable to be replaced with wireless communication links. Furthermore, the emergence of power harvesting devices now

*Correspondence to: Jerome P. Lynch, Department of Civil and Environmental Engineering, University of Michigan, 2350 Hayward St, 2380 G.G. Brown Building, Ann Arbor, MI, 48105, U.S.A.
†E-mail: jerlynch@umich.edu

Received 1 February 2010
Revised 30 June 2010
Accepted 3 July 2010

allows wireless sensors to be deployed without a reliance on grid power [1]. As such, installation and maintenance costs can be reduced from several thousand dollars per sensing channel in the tethered case to under $100 per channel in the wireless case [2]. Wireless sensing networks (WSNs) have also shown great promise because of their ability to process raw sensor data on individual wireless sensing units (WSU) [3]. Significant reductions in network bandwidth, power consumption and distributed storage can be derived by having WSUs convert high-bandwidth raw data streams into low-bandwidth streams of processed results. In dense WSNs where large quantities of measurement data may be generated, these benefits are extremely lucrative.

Early on, researchers focused primarily on decentralized implementations of engineering algorithms that required no communication between WSUs. For example, data processing architectures were developed for embedding stand-alone algorithms into WSUs such as domain transforms (e.g. Fourier, Wavelets), autoregressive model fitting, damage index methods, among many others [4–6]. These embedded data processing methods were shown to be relatively power efficient when compared to the transfer of large tracts of time history data to a central location [4]. However, the lack of data sharing between WSUs prevents these decentralized architectures from autonomously determining system-wide properties (such as mode shapes). Later, researchers moved from decentralized to distributed data processing architectures by leveraging *ad hoc* communication links to exchange data and to coordinate the flow of program execution. For example, Chintalapudi *et al.* [7] present a tiered system where data processing tasks are performed on a distributed network using powerful gateway nodes. This method involves a top-down approach that allows for a flexible and highly abstracted user interface, but in which the computational capabilities of the prolific lower nodes are largely ignored. Other methods involving hierarchical sensing networks that leverage their pervasive lower nodes have also been presented in the literature [8,9]. These techniques can improve network scalability by limiting data size and mitigating data loss, but they rely on a tradeoff between data size and accuracy.

Most recently, an agent-based computing paradigm [10] has emerged in which all WSUs in a homogenous WSN are utilized in a completely parallel and decentralized manner in order to solve complex engineering problems autonomously and without the need for any higher-level coordination. This type of in-network computation has been applied to various SHM problems including modal estimation [11,12], model updating [13], and task scheduling [14]. In general, an agent-based system can be defined as any system in which multiple intelligent agents (in this case, WSUs with computing capabilities) interact directly with each other and with the environment (in this case, any sensors and actuators associated with the SHM system) [15]. In a multi-agent system (MAS), the idea is that a collection of agents, each of which has an incomplete view of its environment and acts according to its own knowledge and set of rules, can be more effective at solving a given problem than a single agent with a complete view of the world. From the perspective of data processing within a WSN, an agent environment can minimize problems associated with power efficiency, data loss, and finite communication ranges while providing a powerful framework for autonomous, in-network processing of data in large-scale WSNs. Additionally, because each WSU is free to communicate with its neighbors, agents can infer spatial information. Finally, because each WSU in an agent-based system has the opportunity to participate equally in any computational task, this framework plays directly to one of the strengths of a WSN: its prolific low-powered processing nodes.

In this paper, the power and flexibility of agent-based data processing in the wireless SHM environment is illuminated through the application of market-based techniques to in-network mode shape estimation. Specifically, by drawing on previous WSN work in both decentralized

DOI: 10.1002/stc

frequency domain decomposition (FDD) [11,12] and market-based resource allocation [14], an algorithm derived from free-market principles is developed through which an agent-based WSN can autonomously and optimally shift emphasis between improving the accuracy of its mode shape calculations and reducing its dependency on any of the physical limitations of a wireless network; namely, processing time, storage capacity, wireless bandwidth, or power consumption. The developed algorithm is validated first in a numerical setting and then by estimating mode shapes using a network of wireless sensor prototypes deployed on the mezzanine balcony of Hill Auditorium, which is located in the University of Michigan campus.

2. MODE SHAPE ESTIMATION USING THE DECENTRALIZED FDD METHOD

The extraction of mode shapes from vibration data has been used by the civil engineering community to calibrate analytical models and to detect severe structural damage. Many mode shape extraction methods have been proposed using output-only structural response data. The FDD method, which was developed by Brincker *et al.* [16], improves upon other output-only approaches by allowing closely spaced modes to be identified with great accuracy. This method works by approximately decomposing the spectral density matrix into a set of single degree of freedom (SDOF) systems. Assuming a broadband input to the system, this can be accomplished by first obtaining an estimate of the output power spectral density (PSD) matrix, $\hat{\mathbf{G}}_{yy}(j\omega)$, for each discrete frequency $\omega = \omega_i$. This matrix is created from an array of frequency response functions (FRFs) calculated using the fast Fourier transform (FFT) from each degree of freedom:

$$\hat{\mathbf{G}}_{yy}(j\omega_i) = \{F_y(j\omega_i)\}\{F_y^*(j\omega_i)\}^{\mathrm{T}} \tag{1}$$

where $F_y(j\omega_i)$ is an array of complex FFT values for each degree of freedom at a given frequency ω_i and $\{F_y^*(j\omega_i)\}^{\mathrm{T}}$ is the complex conjugate transpose (Hermitian matrix) of that array. Then, by taking the singular value decomposition (SVD) of the matrix $\hat{\mathbf{G}}_{yy}(j\omega)$, singular values and singular vectors can be extracted from the PSD matrix as follows:

$$\hat{\mathbf{G}}_{yy}(j\omega_i) = \mathbf{U}_i\mathbf{S}_i\mathbf{U}_i^{\mathrm{H}} \tag{2}$$

where $\mathbf{U}_i = [u_{i1}, u_{i2}, \ldots, u_{im}]$ is a unitary matrix holding m singular vectors, u_{ij}, with each vector term corresponding to the m output degrees of freedom, $\mathbf{S}_i$ is a diagonal matrix holding the scalar singular values s_{ij}, and $\mathbf{U}_i^{\mathrm{H}}$ is the Hermitian transpose of $\mathbf{U}_i$. If a SVD is performed near a modal peak, the vector, u_{i1}, can be interpreted as an estimate of the corresponding mode shape, ϕ_i.

In its traditional centralized implementation, FDD requires that a processing element (e.g. data server) have a significant amount of memory in order to store and manipulate the output PSD matrix for each degree of freedom in the system. For example, if there are 100 sensing nodes in a network, the centralized FDD (CFDD) method requires complex matrix operations to be performed on a 100×100 PSD matrix. Because memory availability is scarce and processing power is limited within a WSN, a decentralized FDD (DCFDD) method has been developed [11].

In the DCFDD approach, each WSU first collects a consistent set of time history acceleration data that is converted into an FRF using an embedded FFT algorithm. Then, an in-network decentralized peak picking algorithm is employed to look for system-wide consensus in identified modal frequencies. Once the entire WSN is apprised of the global modal frequencies,

DOI: 10.1002/stc

each WSU can transmit its individual FFT results at each frequency of interest to the next WSU in a pre-determined chain. Using this data, each receiving WSU can construct a two-degree of freedom output PSD matrix for each picked frequency using the two sets of FFT results in its possession. Then, each receiving WSU performs a SVD on the resulting 2×2 PSD matrices, extracting a set of two-node mode shapes from the singular values corresponding to each modal frequency. Finally, all these two-node mode shapes are shared throughout the WSN where they can be 'stitched' together to form global mode shapes of the structural system. As presented in [11], this decentralized approach reduces the amount of data to be transmitted by two orders of magnitude.

While WSNs employing the DCFDD method have been shown to be capable of creating accurate mode shape estimates, there are two major drawbacks to this method. The first disadvantage is that all global mode shapes that are determined using the DCFDD method are merely linear combinations of two-node mode shapes calculated locally between overlapping pairs of WSUs. As such, the network topology used to create the DCFDD computational chain can have a potentially large impact on the accuracy of the mode shape estimates. Specifically, two-node mode shapes are prone to error when one of the nodes is near or at a zero-point in the mode shape. When global mode shapes are being formed by stitching two-node mode shapes together, an inaccurate two-point mode shape has the potential to propagate its error through the entire estimated shape. It is important to note that this effect is largely dependent on the noise floor of the sensors being used. If there is no noise present in the system, the DCFDD mode shape estimates will match the CFDD estimates exactly. However, as the amount of noise in the system increases, the negative impact of the decentralization will increase as well. This is due to the fact that in a centralized implementation, a least-squares effect minimizes the error due to noise across the entire mode shape, whereas a decentralized implementation allows this error to accumulate through each combination of two-node mode shapes. The second major limitation of the DCFDD method is that a fixed network topology must be decided upon before a WSN can be deployed on a physical structure. As such, DCFDD cannot be applied to a given monitoring scenario without *a priori* knowledge of both the monitored structure and the monitoring system to be deployed. Additionally, this restriction means that the DCFDD method is not sufficiently robust in situations where WSUs fail or temporarily lose communication.

2.1. Improvements to the DCFDD method

One way in which the aforementioned limitations of the DCFDD method could be mitigated is by decreasing the degree of computational decentralization inherent to the technique. In other words, instead of forming global mode shapes out of a sequence of two-node mode shapes (Figure 1(a)), the size of the local mode shapes can be increased to three WSUs or larger. This type of change could be implemented within a WSN by requiring two or more (say, $n-1$) WSUs to transmit their FRF information to another WSU on which an $n \times n$ SVD would be performed. These local n-node mode shapes could then be combined by forcing one or more WSUs in a local mode shape to be redundant to another local mode shape. Note that if more than one WSU overlaps between two local mode shapes, some higher-level mode-stitching methodology (e.g. a least-squares approach) must be utilized to average out any differences in the global mode shapes resulting from the multiple overlapping WSUs. From the FDD perspective, this increased computational centrality could improve the quality of the mode

DOI: 10.1002/stc

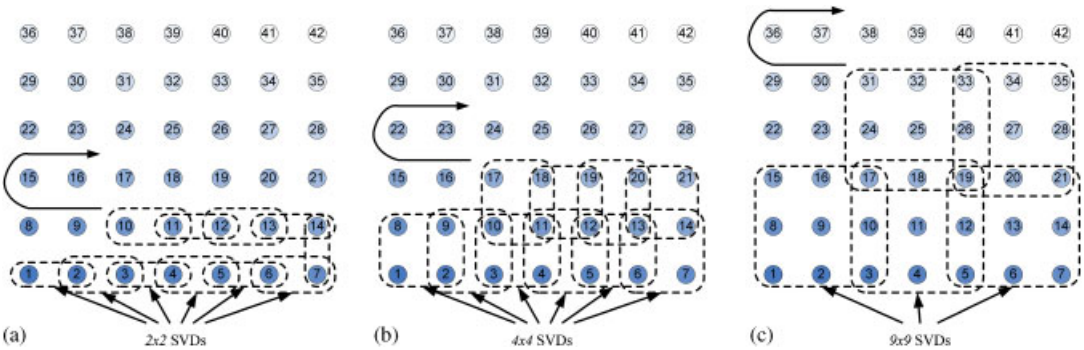

Figure 1. (a) DCFDD topology and two-node SVD sizes from Zimmerman *et al.* [11]; (b), (c) DCFDD topologies and SVD sizes from Sim *et al.* [12] with overlapping four and nine-node clusters, respectively.

shape estimates by avoiding the aforementioned numerical instability possible in the original DCFDD implementation.

A powerful strategy for improving the DCFDD method was recently proposed and implemented in simulation by Sim *et al.* [12]. In this work, global mode shapes are created from a set of local mode shapes by leveraging topologies with increasingly larger sets of overlapping WSUs (Figure 1(b), (c)). By minimizing the error between stitched and reference global mode shapes, the authors found that sufficiently large local groups and multiple overlapping WSUs contribute to more reliable mode shape estimates than were possible with the two-node mode shapes utilized in the original DCFDD method. However, this approach is still based on an *a priori* topology assignment, making it only slightly more robust than the original DCFDD method. Also, this method may require either more communication or more computation than the original DCFDD method, as a subset of WSUs will have to either transmit their data more than once or compute more than one SVD. If computation is more convenient than communications, Sim *et al.* [12] propose the use of the Eigensystem Realization Algorithm (ERA) or the Natural Excitation Technique (NExT) methods in conjunction with the DCFDD methodology to minimize communications at the cost of computational demand.

In general, adopting any DCFDD strategy that generates local modes with three or more nodes will require a trade-off relative to the original 2-node DCFDD methodology: as the size, n, of the local mode shape estimates increases, the amount of time required to complete the necessary $n \times n$ SVD computations will grow faster than at a linear rate (typically by a 2nd or 3rd order polynomial function). Similarly, the total amount of embedded memory required to store a PSD matrix within the WSU memory bank grows with n^2.

3. MARKET-BASED FREQUENCY DOMAIN DECOMPOSITION IN A WSN

As outlined above, it is clear that improvements to the DCFDD method can be made by exploring the effects of fewer (and larger) local mode shape estimates. However, it has also been shown that there is a distinct tradeoff between improved mode shape estimates and the amount of scarce resources required to calculate local mode shapes using increasingly larger clusters of WSUs. In this study, we are interested in optimizing over four distinct (but possibly competing)

DOI: 10.1002/stc

performance objectives: (O_1) estimating mode shapes as accurately as possible from dynamic sensor data; (O_2) calculating mode shape estimates as quickly as possible; (O_3) utilizing as little memory as possible; (O_4) maintaining communications that are as reliable as possible. The objective of this study is to develop a robust methodology in which the tradeoffs between these four objectives can be optimally managed in an autonomous and *ad hoc* manner by a WSN.

3.1. Background on market-based optimization

When dealing with a centralized architecture where all processors have full knowledge of the current state of a system, communication between processors is nearly free, and the performance of a given processor is fairly deterministic, a traditional Nash or Pareto approach to optimization could be employed to manage the aforementioned tradeoff between computational accuracy and resource consumption. However, in the case of computationally endowed WSNs where each WSU is only aware of its own state and where communication and computational tasks can be widely non-deterministic, a different, more adaptive approach to optimization that limits *a priori* assumptions (e.g. network topology) is needed. In contrast to the work by Papadimitriou and Yannakakis [17], who suggest a robust closed-form analytical approach to multiobjective optimization that relies on several *a priori* assumptions, the work presented herein purposefully aims to trade the comfort of a closed form solution for the flexibility and power of an adaptive approach. To this end, this study seeks to leverage the workings of a complex system that is optimally controlled in a highly decentralized manner: the free-market economy.

In a free-market economy, scarce societal resources are distributed based on the local interactions of buyers and sellers who obey the laws of supply and demand. These market-based concepts can be naturally incorporated within a MAS like a WSN, where each market agent (i.e. WSU) can act independently based on economic factors. By embedding within each market agent the desire to maximize an individual utility function (focusing on either mode shape accuracy or resource conservation), competing goals can be settled through market means (i.e. supply and demand equilibrium), thereby producing a Pareto optimal allocation of system resources. In the context of this study, WSUs can be modeled as market agents who are looking to trade an optimal amount of scarce system resources (in this case, storage space and processing time) in exchange for a measure of gained utility (in this case, improved mode shape estimates). This idea is not entirely new, as researchers have recently begun to utilize market-based concepts for the control or optimization of other complex systems such as computer networks and parallel computing platforms [18]. Perhaps the greatest benefit of market-based optimization is that it can yield a Pareto optimal solution; a Pareto optimal market is one in which no participant can have a higher utility without causing harm to other participants when reallocating resources [19].

3.2. Market-based frequency domain decomposition

In contrast to the DCFDD method, which uses a pre-defined chain-like topology through which computational tasks (specifically, 2×2 SVD calculations) are distributed (Figure 1(a)), the market-based frequency domain decomposition (MBFDD) technique creates an *ad hoc* tree-like topology through which a set of SVD calculations of varying size can be distributed (Figure 2). Any MBFDD topology can be uniquely defined by simply listing the children of each WSU in a network. This *ad hoc* approach has numerous advantages over both chain-like DCFDD topology formations and approaches using larger computational clusters. First, by expanding

DOI: 10.1002/stc

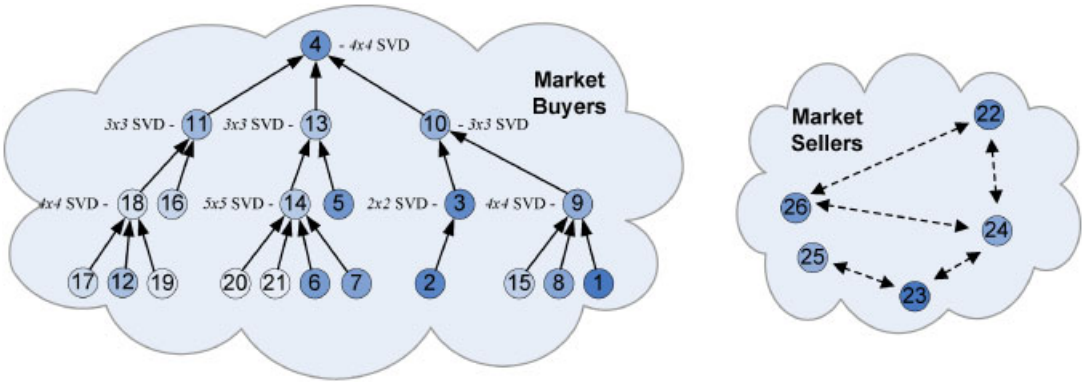

Figure 2. Example MBFDD network topology, buyer–seller framework, and SVD sizes.

the potential size of each local mode shape (i.e. SVD dimension), problems associated with stitching together two-node modes can be greatly mitigated while the accuracy of the global mode shape estimation will improve. Second, this type of optimal *ad hoc* tree creation is not dependent on a predefined topology. Rather, the MBFDD method creates in real-time an optimal tree for mode shape estimation even in the midst of unknown sensor placement, sensor failure, or poor network communication conditions; this is by far its most powerful feature. In lieu of closed form analytical optimization formulations that are limited by their assumptions, these phenomenological but adaptive market-based methods are ideal for WSN resource allocation.

In the MBFDD method developed in this study, all WSUs will either be required to transmit their frequency domain data to another WSU (like WSU 19 in Figure 2), receive frequency domain data (at estimated modal frequencies) from $n-1$ additional WSUs and compute an $n \times n$ SVD (like WSU 4 in Figure 2), or transmit, receive, and compute (like WSU 11 in Figure 2). The purpose of the MBFDD technique, then, is to create an optimal tree-like topology for sending, receiving, and computing dynamic sensor data so as to simultaneously optimize between objectives O_1, O_2, O_3, and O_4. From a market perspective, the utility, U, of a given MBFDD topology can therefore be defined as follows:

$$U(\mathbf{p}, \mathbf{Q}, \mathbf{RSSI}) = \sum_{i=1}^{N} \left[M(p_i) - \alpha \cdot T(p_i) - \beta \cdot S(p_i) + \gamma \cdot \sum_{j=1}^{N} [(Q_{i,j} + Q_{j,i}) \cdot C(\mathrm{RSSI}_{i,j})] \right] \quad (3)$$

where N is the number of WSUs in the network, $\mathbf{p}$ is an N-dimensional vector containing the number of MBFDD children each WSU has, $\mathbf{Q}$ is an $N \times N$ parenthood matrix containing a one in each cell (i,j) where WSU i is a parent of WSU j and zeros elsewhere, **RSSI** is an $N \times N$ matrix containing the radio signal strength indicator (RSSI) values for each wireless connection in the network, $M(p_i)$ is the expected mode shape improvement over the DCFDD case brought about by a MBFDD cluster of size p_i (see Equation (7)), $T(p_i)$ is the increase in computing time relative to the DCFDD case brought about by a MBFDD cluster of size p_i (see Equation (8)), $S(p_i)$ is the increase in storage requirement relative the DCFDD case brought about by a MBFDD cluster of size p_i (see Equation (9)), $C(\mathrm{RSSI}_{i,j})$ is the probability of communication success between WSU i and WSU j (see Equation (10)), and α, β, and γ are weighting parameters that allow for a

DOI: 10.1002/stc

shift of focus between mode shape accuracy, computational speed, storage capacity, and communication reliability. The optimal MBFDD topology is defined by $\mathbf{p}^*$, and $\mathbf{Q}^*$ that maximize $U(\mathbf{p}, \mathbf{Q}, \mathbf{RSSI})$.

Because each WSU has an incomplete view of the state of the WSN as a whole, utility-based decisions leading to this optimal topology must be made through the interaction of individual buyers and sellers. Market sellers in the MBFDD method can be defined as the set of WSUs in the WSN not currently assigned to any action. In a way, these WSUs will be 'selling' their sensor data to one of a number of buyers. Market buyers in this MBFDD method are represented by the set of WSUs currently assigned to either send, receive-compute, or a combination of the two. In Figure 2, all WSUs in the MBFDD tree are market buyers (WSU 1 to WSU 21), while all unassigned WSUs are market sellers (WSU 22 to WSU 26).

3.3. Formulation of buyer-side and seller-side utility functions for MBFDD

It is now necessary to explicitly derive both buyer and seller utility functions associated with each individual market transaction occurring during the creation of the MBFDD topology. For example, a given market buyer, WSU i, can calculate the increase in utility, $\Delta U_B^{i,j}$, it experiences by adding a market seller, WSU j, to its computational cluster by using a weighted combination of the expected improvement in modal assurance criteria (MAC) [20] value, $\Delta M(p^i)$, the increase in computational time, $\Delta T(p^i)$, and the increase in storage capacity, $\Delta S(p^i)$, brought about by its move from SVD cluster size p^i-1 to SVD cluster size p^i, as well as the degree of reliability of the communication link, $\Delta C(\mathrm{RSSI}_{i,j})$. As such, $\Delta U_B^{i,j}$ can be defined as follows:

$$\Delta U_B^{i,j} = \Delta M(p^i) - \alpha \cdot \Delta T(p^i) - \beta \cdot \Delta S(p^i) + \gamma \cdot \Delta C(\mathrm{RSSI}_{i,j}) \tag{4}$$

A given market seller, WSU j, can represent the increase in utility, $\Delta U_S^{i,j}$, that it experiences by joining the computational cluster governed by market buyer, WSU i, using the degree of reliability associated with the communication link, $\Delta C(\mathrm{RSSI}_{i,j})$. $\Delta U_S^{i,j}$ is defined as follows:

$$\Delta U_S^{i,j} = \gamma \cdot \Delta C(\mathrm{RSSI}_{i,j}) \tag{5}$$

allowing us to write:

$$U = \sum_{i=1}^{N} \sum_{j=1}^{N} [Q_{i,j} \cdot \Delta U_B^{i,j} + Q_{j,i} \cdot \Delta U_S^{i,j}] \tag{6}$$

where $Q_{i,j}$ is set to one if WSU i is a parent of WSU j and zero otherwise (note, $Q_{i,j} \neq Q_{j,i}$).

In any FDD calculation, $\Delta M(p)$ can be thought of as the expected improvement in MAC value brought about by moving one WSU from a cluster of 2 WSUs (we will call this Cluster A) into an existing $p-1$ WSU cluster (Cluster B), thus creating a new p-WSU cluster (Cluster C). Using experimental data simulated using a simple analytical model of a 3-m long cantilevered beam (Figure 3(a)), the average improvement in MAC value gained by estimating a mode shape directly using an $p \times p$ SVD (from Cluster C) rather than stitching together mode shapes estimated using both an $(p-1) \times (p-1)$ SVD (from Cluster B) and a 2×2 SVD (from Cluster A) can be determined (Figure 3(b)). Because we expect the value of $\Delta M(p)$ to constantly decrease with respect to p^i and to plateau at a near zero-value as p becomes large, it is found that each of the curves in Figure 3(b) (representing varying noise levels between 0.1% RMS and 50% RMS) can be modeled by an easily computable exponential function as follows:

$$\Delta M(p) = A \cdot \mathrm{e}^{-\lambda \cdot p} \tag{7}$$

DOI: 10.1002/stc

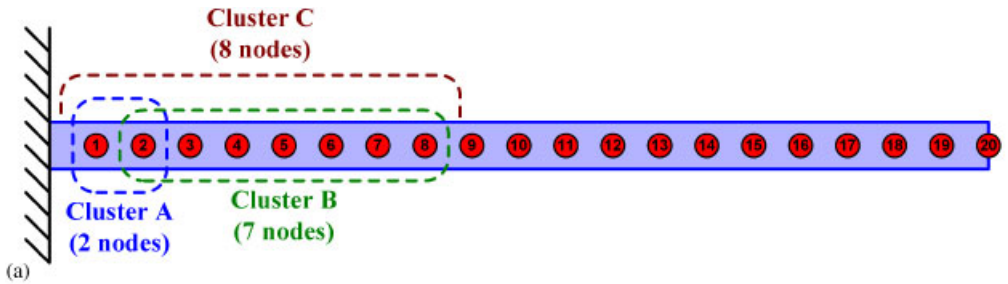

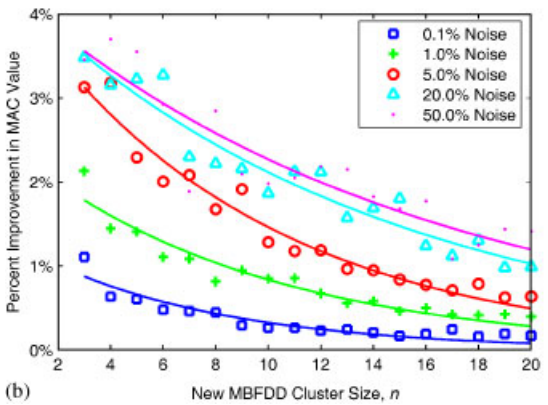

Noise Level	A	λ	R^2
0.0%	0.0000	0.0000	0.93
0.1%	0.0133	0.1406	0.86
0.5%	0.0251	0.1311	0.92
1.0%	0.0246	0.1079	0.92
5.0%	0.0433	0.1087	0.96
10.0%	0.0497	0.1022	0.94
20.0%	0.0437	0.0724	0.93
30.0%	0.0439	0.0670	0.94
50.0%	0.0432	0.0642	0.84

(c)

Figure 3. (a) Potential SVD clusters for mode shape estimation (Clusters A and B vs Cluster C); (b) percent improvement in MAC value, for sensor data with varying noise levels, brought about by increasing computational cluster size; and (c) accompanying analytical regressions (for use with Equation (7)).

where the noise-specific values for A and λ are determined using an exponential regression (they are tabulated in Figure 3(c)). Note that because the benefit of increasing cluster size is experimentally determined to be independent of the mode of interest, the data that were used to develop the regressions in Figure 3 represent an average over the first four modes of the simulated beam. Also note that increased MAC improvement becomes indistinguishable with noise levels at or above 50% RMS. It is also important to note that the regression in Equation (7) is only valid if the cluster being added to already contains at least two nodes; as such, we define $\Delta M(1) = \Delta M(2) = 0$.

In this study, $\Delta T(p)$ represents the expected increase in processing time required to compute a $p \times p$ SVD instead of an $(p-1) \times (p-1)$ SVD. An empirical trend for this parameter can be established by looking at the average time required to complete an SVD of a given size on a WSU microprocessor. Using data taken from an 8-MHz Atmel ATmega128 (a common microcontroller used by the WSN community), a second-order polynomial can model $\Delta T(p)$:

$$\Delta T(p) = (6.14 \times 10^{-3}) \cdot \; p^2 - (0.14 \times 10^{-3}) \cdot p \tag{8}$$

The value of $\Delta S(p)$ in any MBFDD calculation represents the increased number of bytes of storage required to compute a $p \times p$ SVD instead of a $(p-1) \times (p-1)$ SVD. Unlike $\Delta M(p)$ and $\Delta T(p)$, the value of $\Delta S(p)$ is deterministic, as any $p \times p$ SVD computation requires storage of a

DOI: 10.1002/stc

$p \times p$ matrix of complex single precision floating point values (i.e. 8 bytes). $\Delta S(p)$ can be modeled as:

$$\Delta S(p) = 8 \cdot p^2 - 8 \cdot (p-1)^2 = 16 \cdot p - 8 \tag{9}$$

Like $\Delta S(p)$, it is possible to model $\Delta C(\text{RSSI})$ using an analytical expression. This expression is dependent on two parameters, which are correlated to the specific wireless platform: (1) the radio signal strength indicator (RSSI), which correlates to the strength of a wireless connection, and (2) the probability of a communication link with a perfect RSSI failing due to unforeseen circumstances, p_{CF}. Within the MBFDD framework, the RSSI parameter can be gathered directly from the radio interface for a given buyer–seller connection, while p_{CF} is a platform-specific quantity that is usually quite low. In this study, p_{CF} is conservatively taken to be 0.1, although a set of experimental tests on the wireless platform used in this study show it to be much smaller (<0.01). Because wireless transceivers have a narrow band of signal strength (in this case, between RSSI values of -50 and -30 dB) outside of which the probability of packet reception is either 0 or p_{CF}, $\Delta C(\text{RSSI})$ can be defined as a sigmoid function:

$$\Delta C(\text{RSSI}) = \frac{1 - p_{\text{CF}}}{1 + e^{-0.4(40+\text{RSSI})}} \tag{10}$$

3.4. MBFDD auction-based topology creation

Having developed a framework for calculating the utility of a given buyer–seller connection, it is now possible to create a methodology with which WSUs can buy and sell processing time and storage space for the estimation of optimal mode shapes using the MBFDD method. By expanding on the fundamental principles of an auction, the following procedure is proposed to form a computational topology that optimizes the consumption of scarce system resources (Figure 4):

1. The MBFDD topology creation algorithm is initialized by assigning the generic FDD task (at a subset of chosen frequencies) to one available WSU (chosen at random). This WSU becomes the root of the MBFDD tree. An example MBFDD tree and its resulting buyer/seller delineation for a small WSN can be seen in Figure 4(a). Note that in this figure, two WSUs (WSU 5 and WSU 4) have already been assigned to the root (WSU 2).
2. Each WSU already assigned to a position in the MBFDD tree (i.e. each buyer) broadcasts its 'job offer' to whichever sellers are within communication range. These buyer broadcasts occur one at a time, traversing the MBFDD tree in a depth-first fashion starting with the root (e.g. WSU 4, 11, 18, 17, 12, 19, 16, 13, etc. in Figure 2). In this way, a connection is made between each potential buyer and seller in the market. Figure 4(b) demonstrates this process, with sequential broadcasts from WSUs 2, 5, and 4. Note, not one WSU is capable of communication with all other WSUs in the network.
3. Upon receiving a bid from a buyer WSU i, each seller WSU j will calculate the utility, $\Delta U_S^{i,j}$, that it would gain by accepting the buyer's bid. It will then transmit this utility information to the buyer, using a randomized backoff to avoid packet collision. Example seller utilities for each buyer–seller combination can be found in Figure 4(c). Note a correlation between $\Delta U_S^{i,j}$ and communication distance.
4. After a buyer WSU i broadcasts its 'job offer' (step 2), it will wait for a period of time to ensure that all utility values, $\Delta U_S^{i,j}$, have arrived from the sellers. A buyer will then calculate the utility, $\Delta U_B^{i,j}$, it will gain from adding an additional WSU to its SVD cluster. Example buyer utilities for each buyer–seller combination can be found in Figure 4(d).

DOI: 10.1002/stc

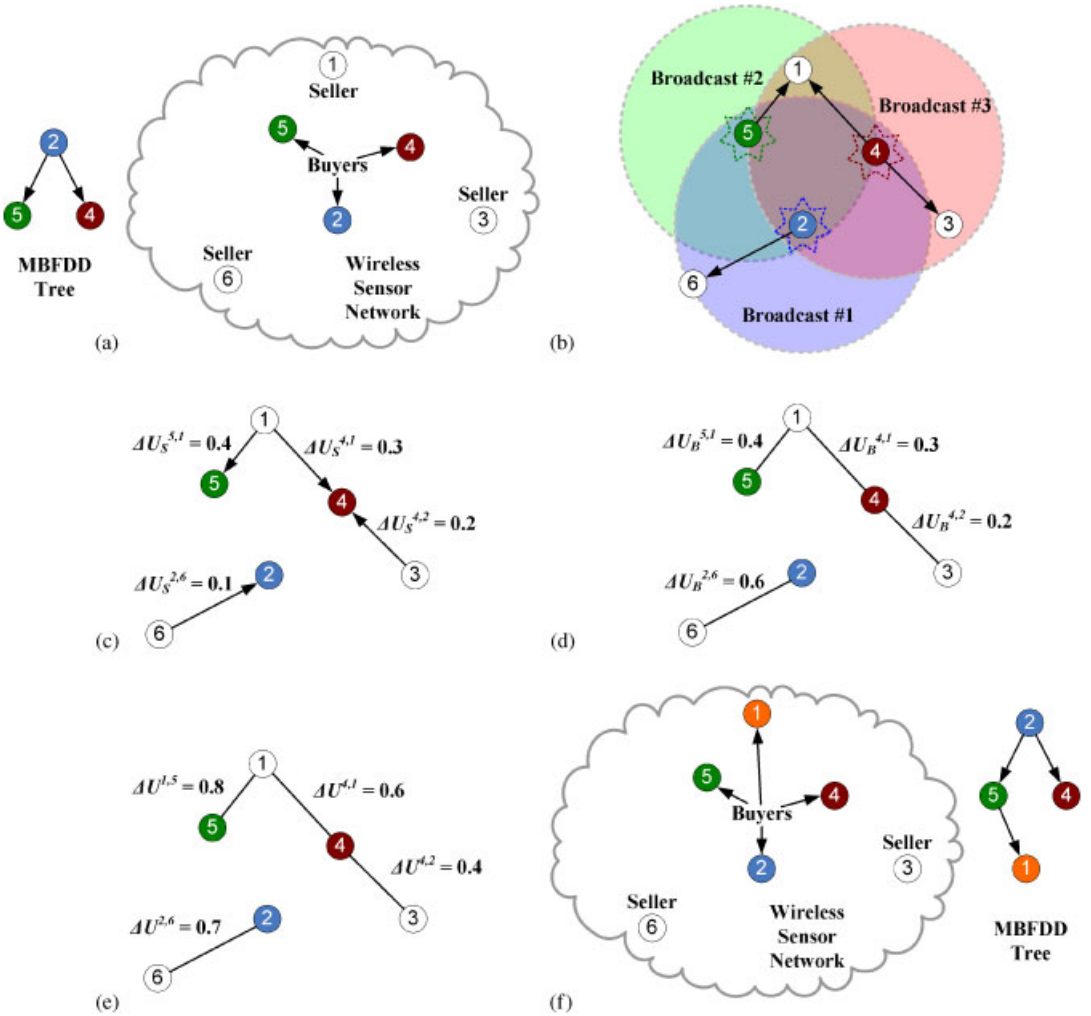

Figure 4. MBFDD algorithm: (a) example MBFDD tree (mid-creation) and buyer/seller delineation; (b) buyer broadcast; (c) seller utility determination; (d) buyer utility determination; (e) total market utility; and (f) updated MBFDD tree and buyer/seller delineation.

Note that buyer utilities are correlated to the size of the buyer's existing SVD cluster, but currently unformed clusters represent a buyer utility of 0.

5. For each seller utility it receives, a buyer will then calculate the expected total market utility, $\Delta U^{i,j} = \Delta U_B^{i,j} + \Delta U_S^{i,j}$, gained from moving forward with that buyer–seller relationship. Figure 4(e) shows the profit calculated from $\Delta U_B^{i,j}$ and $\Delta U_S^{i,j}$. Note that the highest utility is generated between WSU 5 and WSU 1.
6. After all seller information has been received, the buyer will determine the seller with which it can generate the greatest market utility, and will pass that information (including buyer identification number, seller identification number, and buyer–seller $\Delta U^{i,j}$) to the next buyer in a depth-first traversal of the MBFDD tree. If, however, the greatest market

DOI: 10.1002/stc

utility generated by the current buyer is less than the market utility generated by a previous buyer–seller pair, the current buyer will pass along the information relating to the previous buyer–seller instead. In this way, information regarding the buyer–seller combination that generates the greatest market utility at a given time step will propagate through the MBFDD tree, eventually ending back at the root WSU (WSU2 in Figure 4).

7. After all buyers have completed the broadcast/bid process, the root WSU will command the buyer involved in the maximum utility connection (using the MBFDD tree structure for communication) to add the seller WSU associated with the maximum utility to its computational cluster. This step is visualized in Figure 4(f), where the maximum utility pair of WSUs (WSU 5 and WSU 1) are paired in the tree.
8. Steps 2–7 are repeated until no unassigned (seller) WSUs remain in the network.

Using this algorithm, a MBFDD computational tree can be created such that the overall utility, $U(\mathbf{p}, \mathbf{Q}, \mathbf{RSSI})$, of the market is maximized. The weighting parameters, α, β, and γ, render the framework capable of optimally adapting to shifting computing needs or resource limitations within a WSN. For example, assume that it is absolutely essential that a particular mode shape estimate be as accurate as possible. Without any reprogramming of the sensing network, the network can simply assign near-zero values to α, β, and γ, in order to reflect the added emphasis on improving computational accuracy. Similarly, increasing values of α can be used to emphasize computational speed, β to stress storage restrictions, and γ to stress communication reliability.

4. SIMULATED BEAM TESTBED AND RESULTS

In order to validate the market-based task assignment methodology proposed in this study, the four performance metrics (M_1 through M_4) outlined in Section 3 must be evaluated. Because it is necessary to examine the performance of the MBFDD algorithm over a statistically large number of runs and under a variety of different sensor noise conditions, it is decided to first utilize a simulated cantilever beam as a testbed. The beam (Figure 3(a)) is 3 m long and has a flexural rigidity (EI) of 215.2 kN m^2. In simulation, the cantilevered beam is monitored by 20 WSUs, each measuring vertical acceleration and positioned at equal spacing across the length of the beam. This beam is excited with a broadband input by impulsing it at its tip, thereby yielding its first four vibration modes at 2.9, 18.4, 51.4, and 100.8 Hz, respectively. In the simulated portion of this study, the tuning parameters α, β, and γ are examined for their ability to shift the priority of the MBFDD methodology from mode shape accuracy to: (1) high computational speed (at high values of α); (2) low storage requirements (at high values of β); and (3) high communication reliability (at high values of γ). To achieve this goal, the WSN is repeatedly asked to estimate the first four mode shapes using the MBFDD method with varying values of α, β, and γ. Furthermore, three noise levels (1.0, 10.0, and 50.0% RMS) are considered.

In this study, MBFDD mode shape estimates are compared with CFDD estimates using the MAC [20]. By taking the difference between the average MBFDD MAC value and the average CFDD MAC value for a given mode shape and noise level, we can generate a MAC error between the MBFDD estimates and the CFDD estimates. Using this method for quantifying mode shape error, Figure 5(a, b) displays the average accuracy and computational speed of the MBFDD algorithm when run with varying assignments to α and using varying levels of sensor noise. It is

DOI: 10.1002/stc

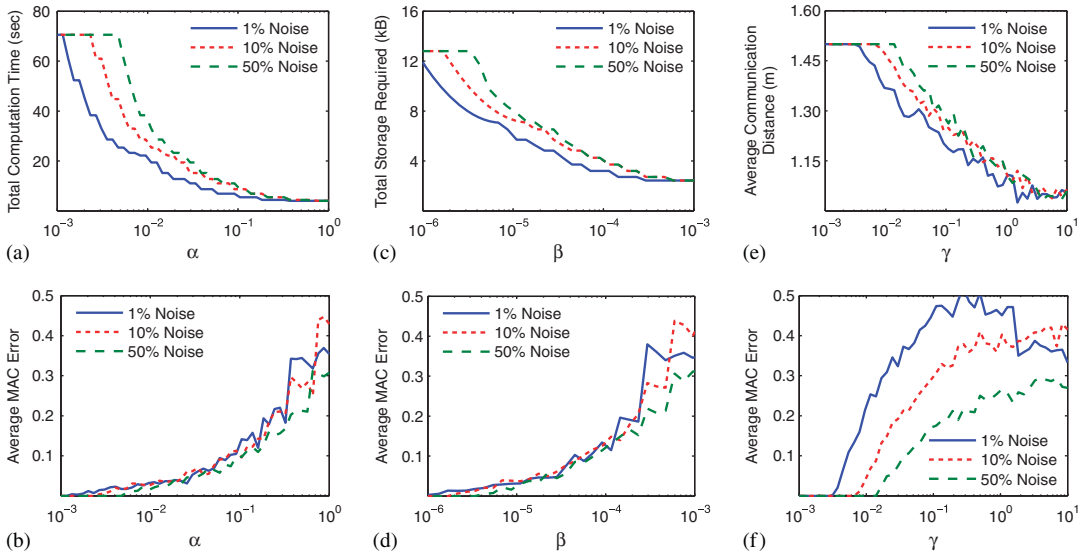

Figure 5. (a), (b) Total computation time and average MAC error vs weighting parameter α; (c), (d) total storage requirements and average MAC error vs weighting parameter β; and (e), (f) average communication distance and average MAC error vs weighting parameter γ for the MBFDD method applied to the numerical cantilever testbed for three different levels of noise: 1, 10, and 50%.

clear that not only is the MBFDD method capable of creating a very accurate mode shape estimate, but it can also effectively utilize the tuning parameter α to discriminate between an emphasis on mode shape accuracy and an emphasis on computational speed. Similarly, Figure 5(c, d) displays the average accuracy and storage requirements of the MBFDD algorithm when run with varying assignments to β and using varying levels of sensor noise. In this suite of figures, it can be seen that the MBFDD method can effectively utilize the tuning parameter β to discriminate between an emphasis on mode shape accuracy and an emphasis on required data storage.

In this investigation, the effect of communication quality on the MBFDD topology is evaluated by looking at the average (geometric) distance between communication links in the MBFDD tree. Because RSSI is correlated to distance between transmitter and receiver (assuming line-of-sight), it follows that WSUs that are farther from one another on the cantilever will have lower mutual RSSI values; lower RSSI values indicate decreased communication reliability. Figure 5(e, f) displays the average accuracy and communication distance of the MBFDD algorithm when run with varying assignments to γ and using varying levels of sensor noise. It is clear that the MBFDD method is capable of discriminating between an emphasis on mode shape accuracy and an emphasis on communication reliability by utilizing the tuning parameter γ. It is interesting to note that at values of γ greater than 1.0, we actually see a decrease in mode shape error. This is because at these large values of γ, output from the MBFDD algorithm approaches the DCFDD topology (i.e. the MBFDD tree is merely a sequential chain of sensors running the length of the cantilever). Because of the simplicity of this beam example, this sequential ordering actually happens to produce improved results at low noise levels for certain mode shapes. However, this phenomena does not extend to more complex examples.

DOI: 10.1002/stc

5. THEATRE BALCONY TESTBED AND RESULTS

Having validated the proposed MBFDD algorithm on a simulated testbed, a physical structure is now required to evaluate algorithmic performance in a real-world scenario. For this purpose, the mezzanine balcony of Hill Auditorium (Ann Arbor, MI) (Figure 6(a)) is instrumented with 15 wireless sensing prototypes located in rows 1, 3, and 5 of each of the five sections of the mezzanine balcony (Figure 6(b)). The dimensions of the balcony are 43 m wide by 19 m deep. The sensing prototype used in this study is the *Narada* WSU, developed at the University of Michigan [21]. This WSU is powered by an 8-MHz Atmel ATmega128 microprocessor. It is supplemented by 128 kB of external SRAM and utilizes the four channel, 16-bit ADS8341 ADC for data acquisition. The *Narada*'s wireless communication interface consists of the Chipcon CC2420 IEEE 802.15.4-compliant transceiver. This prototype is typically powered by six AA batteries. Each *Narada* WSU is used to monitor either a PCB Piezotronics 3801D1FB3G MEMS capacitive accelerometer or a Crossbow CXL02LF1Z MEMS capacitive accelerometer, oriented to monitor the vertical acceleration of the balcony. The sensitivity of the PCB accelerometer is 0.7 V/g and its full-scale range is 3 g, peak-to-peak. The sensitivity of the Crossbow accelerometer is 1.0 V/g and its full-scale range is 2 g, peak-to-peak. To improve the performance of the WSN, a signal conditioning circuit [22] is included with each sensor to both amplify and band pass (0.02–25 Hz) acceleration response data before connecting to the wireless sensor's ADC.

During the course of testing, each *Narada* WSU is programmed with the MBFDD algorithm, and asked to autonomously form computational clusters for mode shape estimation using varying values of α, β, and γ. Then, a series of 16 dynamic tests are run using a variety of loading scenarios including frequency chirps using an APS Electro-Seis 113 modal shaker, impulse loads

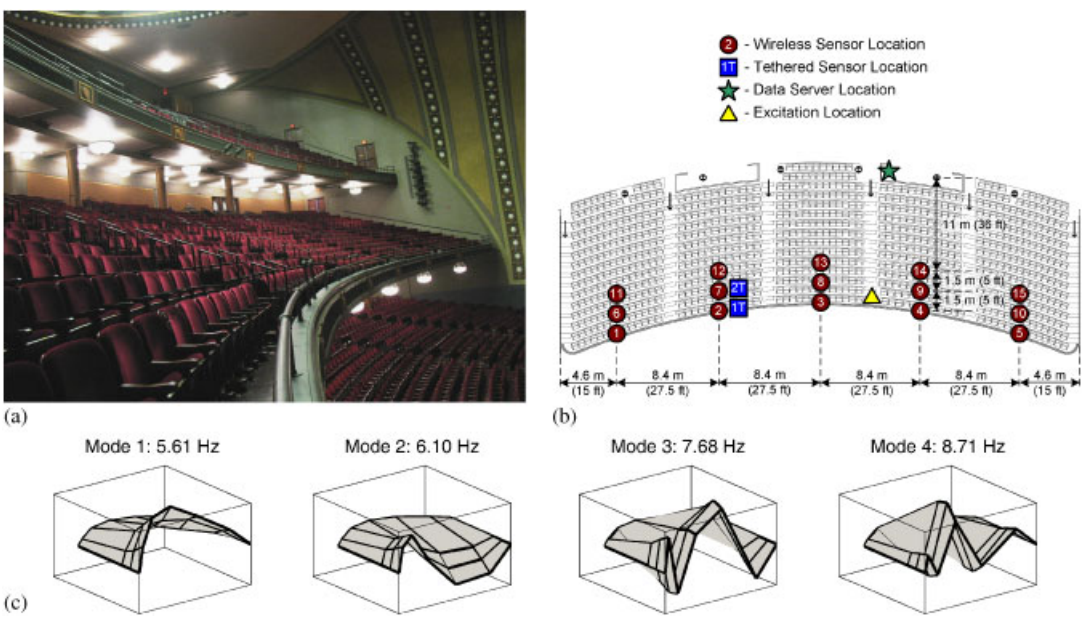

Figure 6. (a) Hill Auditorium mezzanine balcony; (b) location of wireless and tethered accelerometers; and (c) first four mode shapes measured by CFDD method.

DOI: 10.1002/stc

with a Dytran 5803A modal hammer, and heeldrops performed by a single person weighing 82 kg (180 lb). Each set of dynamic testing data was used to generate MBFDD mode shapes at four predetermined frequencies (5.61, 6.10, 7.68, and 8.71 HZ), corresponding to the first four modes of the system. Mode shapes calculated by the CFDD method at these four frequencies can be seen in Figure 6(c).

As was the case with the simulated testbed, the MBFDD validation performed on the theater balcony focuses on the tuning parameters α, β, and γ, and their ability to shift the priority of the MBFDD methodology from mode shape accuracy (at low values of α, β, and γ) to high computational speed (at high values of α), low storage requirements (at high values of β), and high communication reliability (at high values of γ). Experimental results seen in Figure 7(a) display the average MAC error (relative to a CFDD estimate) and average computational speed of the MBFDD algorithm when run with a suite of different values of α (varying between 10^{-3} and 10^{0}). Similarly, Figure 7(b) displays the average MAC error (relative to a CFDD estimate) and average storage requirements of the MBFDD algorithm when run with varying values of β (varying between 10^{-6} and 10^{-3}). These results confirm that the MBFDD method is not only capable of creating a very accurate mode shape estimate (at low values of α and β), but that it

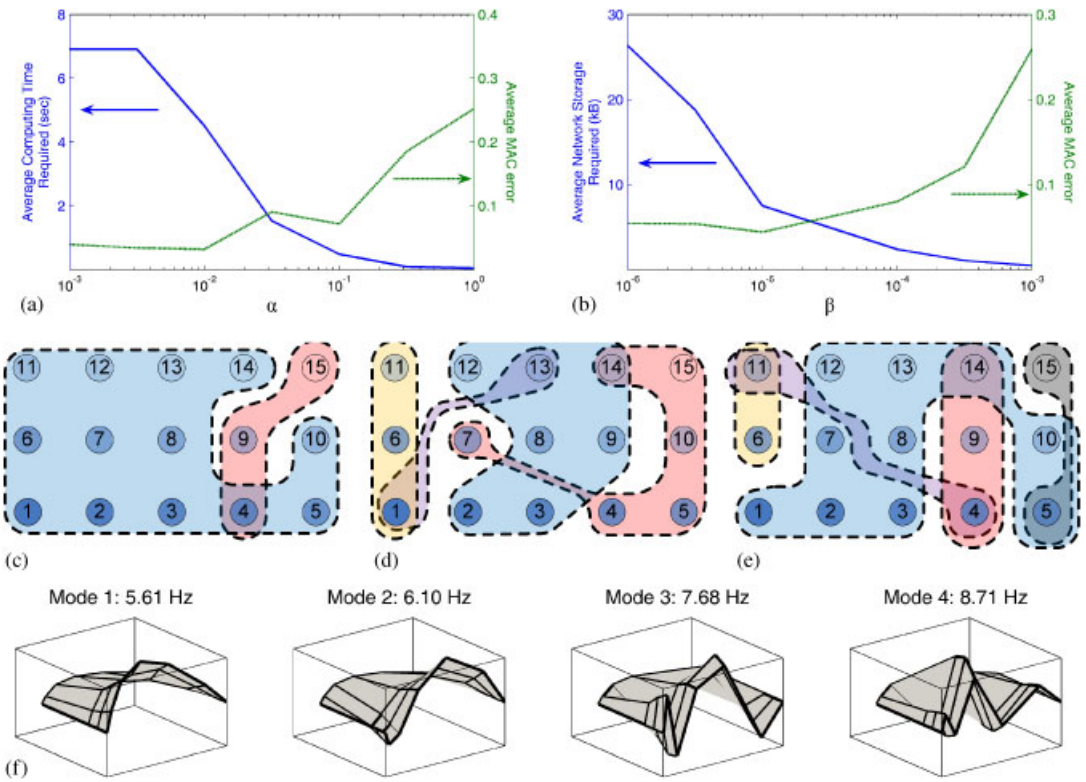

Figure 7. (a) Experimentally determined tradeoff between MBFDD computing time and mode shape error shown for increasing values of α. (b) Experimentally determined tradeoff between MBFDD network storage and mode shape error shown for increasing values of β. Experimentally created MBFDD clusters shown for values of γ equal to (c) 10^{2}, (d) 10^{5}, and (e) 10^{7}. (f) First four experimentally determined mode shapes using the MBFDD method where α is equal to $10^{-1.5}$.

DOI: 10.1002/stc

can also effectively utilize these tuning parameters to discriminate between an emphasis on mode shape accuracy and an emphasis on increased computational speed or decreased storage requirements.

The last MBFDD validation performed on the theater balcony focuses on the tuning parameter γ. In contrast to the validation of α and β, γ can be shown to be functioning as designed if as the value of γ is increased, the average communication distance between WSUs in each MBFDD cluster will decrease. Figure 7(c–e) shows the final clusters that were formed using three increasing values of γ (10^2, 10^5, and 10^7) and speak to the MBFDD method's ability to utilize this tuning parameter to emphasize communication reliability through the creation of spatially localized computational clusters. It should also be noted that γ can be used as a means of localizing computational clusters for other purposes. For example, in a SHM system, local clusters versus more global clusters could be used for more local-scale investigation of structural response data for damage detection. Mode shapes calculated by the MBFDD method can be seen in Figure 7(f).

6. SUMMARY AND CONCLUSIONS

In this study, the power and flexibility of agent-based data processing in the wireless structural health monitoring environment is illuminated through the application of market-based techniques to in-network mode shape estimation. Specifically, by drawing on previous wireless sensor work in both DCFDD and market-based resource allocation, an algorithm derived from free-market principles is developed through which an agent-based wireless sensor network can autonomously and optimally shift emphasis between improving the accuracy of its mode shape calculations and reducing its dependency on any of the physical limitations of a wireless network: processing time, storage capacity, and communication reliability. The resulting MBFDD algorithm is validated first in a numerical setting and then by estimating mode shapes using a network of wireless sensor prototypes deployed on the mezzanine balcony of Hill Auditorium, located on the University of Michigan campus. It is shown that the proposed method is capable of autonomously forming a computational topology that allows a network of wireless sensors to not only improve upon the mode shape estimates of the DCFDD technique but also to optimally distinguish between multiple resource constraints or objectives. Using the weighting parameters α, β, and γ, this market-based method is experimentally shown to be capable of managing a changing emphasis between mode shape accuracy, computational speed, storage requirements, and wireless communication reliability. While this study focused on these specific WSN resources, the MDFDD method is quite powerful in that it can easily consider other resources (e.g. battery power, etc.) by explicitly including them in the market utility functions.

ACKNOWLEDGEMENTS

The authors acknowledge the assistance provided by Junhee Kim, Sean O'Connor, and Kurt Thoma at the University of Michigan. This work was supported by the US Office of Naval Research (Contracts N00014-05-1-0596 and N00014-09-C0103). Additional support has been provided by the National Science Foundation through Grant 0726812. The authors also thank Mr. Sung-Han Sim and Professor Bill Spencer, Jr. from the University of Illinois Urbana-Champaign for valuable discussions centered on DCFDD methods implemented in WSNs.

DOI: 10.1002/stc

REFERENCES

1. Casciati F, Rossi R. A power harvester for wireless sensing applications. *Structural Control and Health Monitoring* 2007; **14(**4):649–659.
2. Lynch JP, Loh KJ. A summary review of wireless sensors and sensor networks for structural health monitoring. *The Shock and Vibration Digest* 2006; **38**(2):91–128.
3. Spencer BF, Ruiz-Sandoval ME, Kurata N. Smart sensing technology: opportunities and challenges. *Journal of Structural Control and Health Monitoring* 2004; **11**:349–368.
4. Lynch JP, Sundararajan A, Law KH, Kiremidjian AS, Carryer E. Embedding damage detection algorithms in a wireless sensing unit for operational power efficiency. *Smart Materials and Structures* 2004; **13**:800–810.
5. Hashimoto Y, Masuda A, Sone A. Prototype of sensor network with embedded local data processing. *Smart Structures and Materials Conference*, San Diego, CA, 2005.
6. Cheung A, Kiremidjian AS, Sarabandi P. A framework for damage diagnosis on civil structures using rotation measurements. *7th International Workshop on Structural Health Monitoring*, Stanford, CA, 2009.
7. Chintalapudi K, Paek J, Gnawali O, Fu TS, Dantu K, Caffrey J, Govindan R, Johnson E, Masri S. Structural damage detection and localization using NetSHM. *5th International Conference on Information Processing in Sensor Networks*, Nashville, TN, 2006.
8. Gao Y. Structural health monitoring strategies for smart sensor networks. Department of Civil and Environmental Engineering, University of Illinois, Urbana-Champaign, IL, 2005.
9. Nagayama T, Spencer BF, Agha GA, Mechitov KA. Model-based data aggregation for structural monitoring employing smart sensors. *3rd International Conference on Networked Sensing Systems*, Chicago, IL, 2006.
10. Ruiz-Sandoval M. *Smart Sensors for Civil Infrastructure Systems*. University of Notre Dame: South Bend, IN, 2004.
11. Zimmerman AT, Shiraishi M, Swartz RA, Lynch JP. Automated modal parameter estimation by parallel processing within wireless monitoring systems. *ASCE Journal of Infrastructure Systems* 2008; **14**(1):102–113.
12. Sim SH, Spencer Jr BF, Zhang M, Xie H. Automated decentralized modal analysis using smart sensors. *Structural Control and Health Monitoring* 2010.
13. Zimmerman AT, Lynch JP. A parallel simulated annealing architecture for model updating in wireless sensor networks. *IEEE Sensors Journal* 2009; **9**(11):1503–1510.
14. Zimmerman AT, Lynch JP, Ferrese FT. Market-based computational task assignment within autonomous wireless sensor networks. *IEEE International Conference on Electro/Information Technology*, IEEE, Windsor, Canada, 2009.
15. Russell SJ, Norvig P. *Artificial Intelligence*: *A Modern Approach* (2nd edn). Pearson Education, Inc.: Upper Saddle River, NJ, 2003.
16. Brincker R, Zhang L, Anderson P. Modal identification of output-only systems using frequency domain decomposition. *Smart Materials and Structures* 2001; **10**(3):441–445.
17. Papadimitriou CH, Yannakakis M. On the approximability of trade-offs and optimal access of Web sources. *41st Annual Symposium on Foundations of Computer Science*, IEEE Computer Society, Los Alamitos, CA, 2000.
18. Clearwater SH. *Market-Based Control*: *A Paradigm for Distributed Resource Allocation*. World Scientific Press: Singapore, 1996.
19. Mas-Colell A, Whinston MD, Green JR. *Microeconomic Theory*. Oxford University Press: New York, NY, 1995.
20. Allemang RJ, Brown DL. A correlation coefficient for modal vector analysis. *International Modal Analysis Conference and Exhibit*, Orlando, FL, 1982.
21. Swartz RA, Jun D, Lynch JP, Wang Y, Shi D, Flynn M. Design of a wireless sensor for scalable distributed in-network computation in a structural health monitoring system. *International Workshop on Structural Health Monitoring*, Stanford, CA, 2005.
22. Wang Y. Wireless sensing and decentralized control for civil structures: Theory and implementation. *Department of Civil and Environmental Engineering*, Stanford University, Stanford, CA, 2007.

DOI: 10.1002/stc